

# Toward Active Control of Turbulent Combustion

## — Development of the Demonstration Combustor System —

S. Tachibana, L. Zimmer, T. Yamamoto, Y. Kurosawa, S. Yoshida and K. Suzuki  
*Japan Aerospace Exploration Agency*  
7-44-1 Jindaiji-Higashi, Chofu, Tokyo 182-8522, Japan  
E-mail: tachibana.shigeru@jaxa.jp

March 2, 2004

### Abstract

The purpose of this work is to develop effective active control means for wide-range stable premixed combustors. We are developing a demonstration combustor system which consists of a target combustor, sensors, actuators and controllers by accumulating the knowledge from the results of fundamental studies among the combustion groups of this project. A methane-air premixed swirl-stabilized combustor was applied as the target combustor. The main premixed flame is stabilized by the axial swirler with orifices for secondary fuel injection on the central hub. For the first step, we set two operating conditions, as typical conditions for a lower and a higher outputs, and investigated natural acoustic modes of combustion oscillation. Several control methods were examined on the unstable points of the conditions. A pressure transducer and a chemiluminescence detector were used as sensors and secondary fuel injections in pulsating/non-pulsating modes were applied as an actuator. Since controller is not built in yet, the parameters needed for actuation were manually set at this point. For the lower output condition, the effects of control methods on the reduction of pressure oscillations is discussed. For the higher output condition, the effects of the amount of secondary fuel injection both on the reduction of pressure oscillation and NOx emission are discussed.

## 1 Introduction

Lean premixed combustion has been considered as a promising way to reduce NOx emission and continuous efforts to build it in the real gas turbine system has been exerted. However, the realization has not been completed yet for some reasons. One main drawback that prevents the realization is the instability of premixed flames. To overcome the difficulties, passive controls have been adopted to the development. In recent days, from the point of view of adaptive flexibility of the control, active control strategies have begun to attract attention and has been examined in many works[1]-[6]. The source of the instability is due to the mutual interaction between fluctuations of pressure and heat-release rate. Hence, for sensors and actuators, there are two standpoints corresponding to each of the components of the instability. Usually, pressure transducers and chemiluminescence detectors are used for sensing pressure and heat-release rate respectively. In a similar way, loud speakers and secondary fuel injections are used for the actuation. From the point of view of application to the real-scale combustor, the actuating energy generated by loud speakers may be too low. Consequently, the secondary fuel injection is considered to be the realistic way for the actuation.

In the framework of this project, fundamental studies toward the active control system have continuously been pursued among the combustion groups. Several applications of chemiluminescence information as sensors have been examined by JAXA group[7]. The effects of high-speed secondary fuel injection have been investigated by TIT group[9]. Anti-phase closed loop controls using microphone as a sensor and a loud speaker or periodic secondary fuel injection as actuators have been developed by AGU and NMRI groups[10]. CFD studies over the whole combustion chamber have been done by JAXA CFD group[11]. Our goal in this work is to develop a demonstration combustor

for the active control of combustion instabilities by installing the fundamental components into one. The higher values of inlet temperature and flow rate for the demonstration combustor will make it more difficult to control than the fundamental studies. For instance, the oscillation tends to be high in frequency as the flame temperature increase. NOx emission due to thermal process is strongly dependent on the flame temperature also. Hence, we cannot simply scale the results of fundamental studies into the demonstration combustor, even though many aspects can contribute to it.

In this paper, we start from relatively low power operating conditions ( $T_{in}=500K$ ,  $U_{swl}=12m/s$ ,  $P \sim 30kW$ ), then go to the higher conditions( $T_{in}=700K$ ,  $U_{swl}=90m/s$ ,  $P \sim 200kW$ ). We employ a pressure transducer and a chemiluminescence detector as the sensors and secondary fuel injection as an actuator. The acoustic characteristics of the combustor are analyzed by signals from both sensors. And several ways of actuation by secondary fuel injections are examined. The effects of the fuel injections on the instability and emission characteristics are discussed.

## 2 Experimental setup

### 2.1 Combustion test rig

Fig.1(a),(b) show the picture and the schematic of the combustor system respectively. The system is composed of an air supply, an electric heater, a main fuel mixer, a flame holder and a combustion chamber. The cross-section of the combustion chamber is formed of a square 100 mm on a side. One of the side wall of the most upstream part of the chamber is made of a crystal glass plate so as to optically access the inside of the chamber.

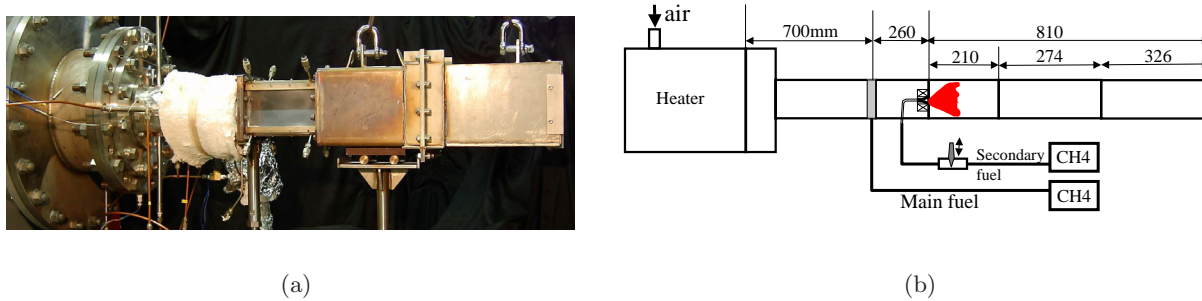


Figure 1: Combustion test rig (a) Picture and (b) Schematic

### 2.2 Flame holder with secondary injection orifices

An axial swirler with secondary injection orifices was installed on the inlet of the combustion chamber. The schematic of the swirler is illustrated in Fig.2. Outer and inner diameters of the swirler are 50mm and 20mm respectively. It is composed of 12 vanes of 30 deg angles and 8 injection orifices of 1.4mm diameter with 30 deg angles. The injection orifices are installed on the central hub. There are two roles for the swirler. One is to hold the main premixed flame by the swirl-induced recirculating flow of high-temperature burnt gas and the other is to actuate secondary fuel injections to control unstable modes of combustion. In the case of pulsating injection, we use Woodward HSC Inc. HSC65A servo-valve by sending the command TTL signal to the servo controller. As a preliminary test to check the response of heat-release rate pulsation against the command signals, a parametric study was performed. In this case, only the secondary fuel was injected from the injection orifices. The main air was supplied as the surrounding air. By sending periodic command signals from a wave generator to the servo controller, pulsation fuel was injected and fluctuating flames were formed. The chemiluminescence emission from the fluctuating flame was detected by Specbox, the chemiluminescence sensor described in the following section. From spectrum analysis

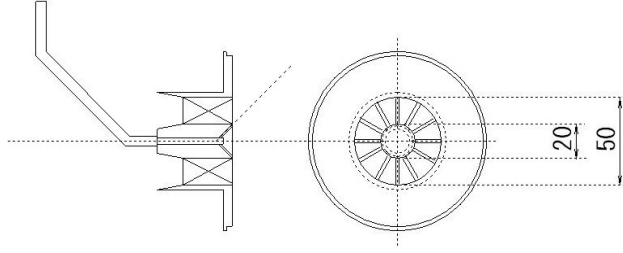


Figure 2: Swirler with secondary injection orifices

of the time series measurements, one can get peak frequencies and peak values of the emission. Fig.3 shows the result of the test. The SNR is defined by the difference in dB between the values of peak and background. Even though the position of the measured peaks coincident well with the imposed frequencies until 700 Hz, SNR decreases rapidly between 200-300 Hz. This implies that we may not have good response beyond the frequency.

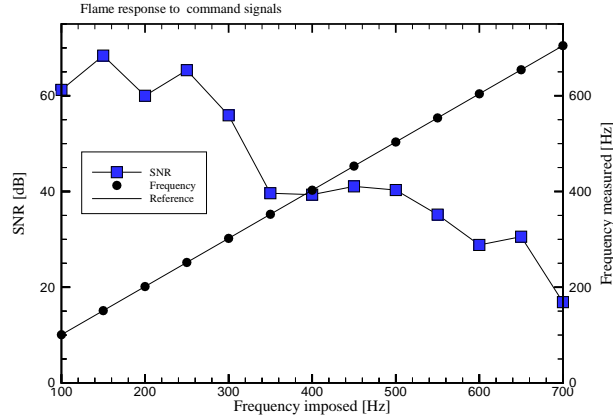


Figure 3: Response of the  $CH^*$  intensity against command signals

### 2.3 Sensing devices

Measurement system for pressure and chemiluminescence is illustrated in Fig.4(a). A pressure transducer (Kulite Semiconductor Products, Inc., Model XTL-190-15G) is placed on the chamber wall at 20 mm downstream from the inlet. A double condenser lens of 300mm focal length is placed on outside of the glass window at the opposite position to the pressure sensor. The collecting light is focused on the optic fiber and transmitted into Specbox. Specbox is the equipment to sift the incident light into four band-passed wavelengths[7]. The components of Specbox are shown in Fig.4(b). In this paper, only  $CH^*$  signal was used as a representation of heat-release rate. A multi-channel data acquisition system (ONO SOKKI, DS-200, Graduo) is used for the simultaneous measurements of pressure and chemiluminescence. Typical sampling frequency is 10kHz for each channel. As described later, only the pressure signal was included as the input for the closed loop control at present. The works to utilize the chemiluminescence information as predictive sensors for combustors are being pursued by our group in parallel[8].

### 2.4 Controller

Even though the plan to build up the controller on board is now in progress, we carried out the closed loop control by manually setting the parameters needed for actuating the valve at this point.

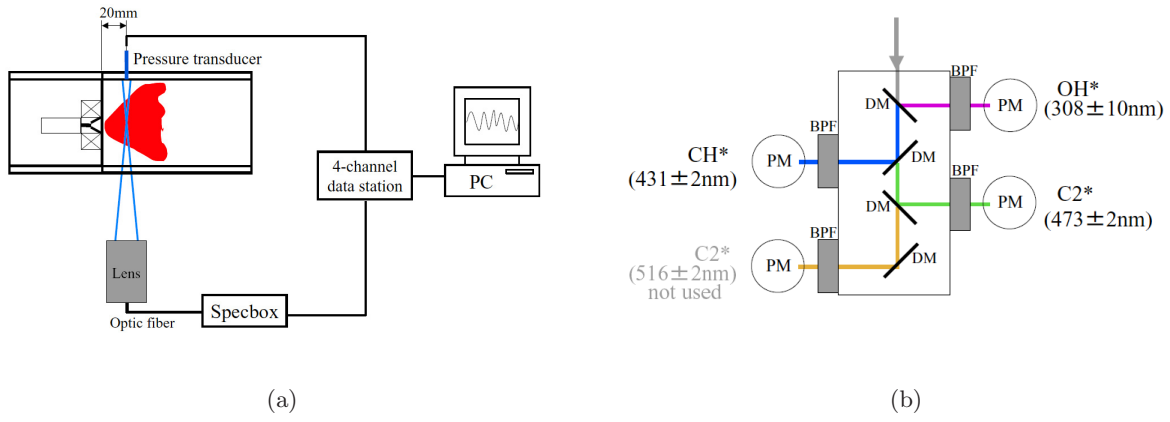


Figure 4: (a) Measurement system, (b) Components of Specbox

The setting parameters are the central frequency of the most unstable mode, the trigger conditions, the time delay and the open width of the pulses.

### 3 Open and closed loop control trials on the lower output condition

An open loop and a closed loop control were examined at the condition of  $T_{in}=500K$ ,  $U_{swl}=12m/s$  and  $L=810mm$ . The main reason to choose this condition for the first trial is that the primary frequency of the unstable mode is around 200Hz(as described below) and the valve actuated secondary injection around this frequency seems to be effective from the preliminary tests (see Fig.3). In the following, natural modes of oscillation and the effects of the two strategies of control are discussed.

#### 3.1 Characteristics of the combustion oscillation

Natural modes of oscillation were investigated by increasing main fuel flow rate. As the equivalence ratio increases, combustion oscillation arose at some point. One can notice the occurrence by the change in amplitude of the pressure fluctuations. In Fig.5, it can be seen clearly that the transition occurs at  $\phi_m \sim 0.67$ . Also shown in Fig.5 is the thermo-acoustic correlation integral  $R$  that is defined by analogy with the Rayleigh index as follows:

$$R = \frac{1}{N} \int_{N\tau} p' \cdot I'_{CH^*} dt \quad (1)$$

Here,  $p'$  is pressure fluctuation at wall and  $I'_{CH^*}$  is the accumulated value of  $CH^*$  intensity over the measurement volume (see Fig.4(a)). We made assumptions that the  $I'_{CH^*}$  has a linear dependency on the fluctuations of global heat release rate and the pressure distribution in space is uniform over the volume.  $\tau$  is the time period for one cycle of oscillation.  $N$  is the number of cycles to be averaged. The correlation integrals show similar transition as pressure fluctuations. It indicates that the oscillation is driven by thermo-acoustic interaction.

The power spectra of pressure fluctuations for different equivalence ratios are shown in Fig6. For  $\phi_m = 0.60$ , there is no clear peak in the spectrum. A peak appears at 202Hz for  $\phi_m = 0.66$ , but the value is less than half of those of higher peaks. The higher peaks around 200Hz were found to be corresponding to the 1/4 longitudinal acoustic modes of the combustion chamber. The second highest peaks around 600Hz are corresponding to 3/4 modes of the basic harmonics. The lower peaks around 400Hz and 800Hz are the higher harmonics due to distortion of the basic signal from completely sinusoidal. The frequencies of the peaks shift toward higher values as the equivalence ratio increase. This is due to the increase of flame temperature which results in the amplification of the speed of sound.

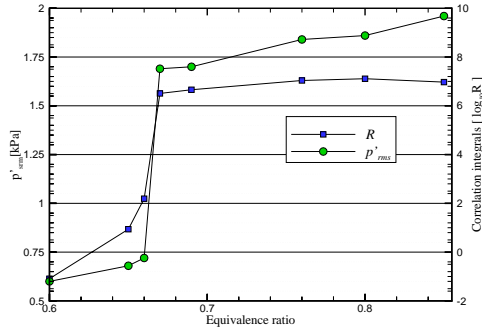


Figure 5: Transition of  $p'_{rms}$  and  $R$

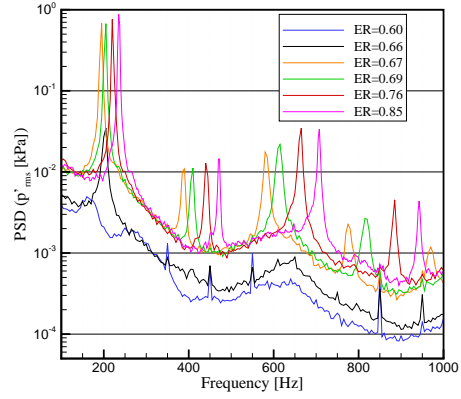


Figure 6: Power spectra of  $p'_{rms}$  (no control)

### 3.2 Effects of controls on the reduction of pressure oscillation

We applied two control methods using secondary fuel injection. One is an open loop control and the other is a closed loop control. In the case of open loop, secondary fuel is injected at a constant flow rate. On the other hand, in the case of closed loop, the valve is actuated in a pulsed mode according to pressure signal. The schematic of the closed loop is shown in Fig.7. Signal from the pressure transducer is put through a band-pass filter and the triggering signal is generated when a positive slope above zero is detected. Then by imposing delay time and open width, the command signal in voltage is generated. The command signal is transformed into current that actuates the solenoid valve. This closed loop of control was carried out by manually setting the central frequency, triggering conditions, delay time and open width. Fig.8 shows a time sequence of pressure fluctuations. During

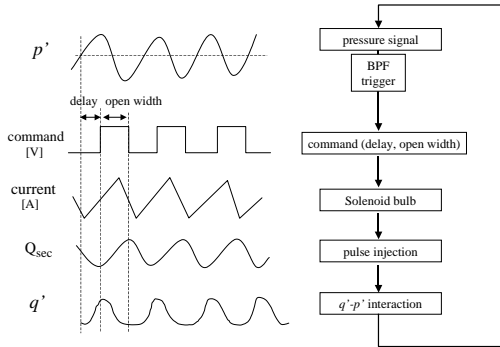


Figure 7: Schematic of closed loop control

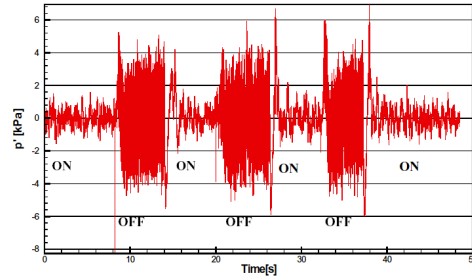


Figure 8: A time sequence of pressure fluctuation

the sequence, the closed loop control was switched on/off repeatedly. The baseline conditions with no secondary injection, thus control-off, is  $T_{in} = 500K$  and  $\phi_t = \phi_m = 0.77$ . In this condition, the natural mode of oscillation is occurring. When the control switch is on, thus when the secondary fuel is injected, total equivalence ratio  $\phi_t$  becomes 0.85 and the amount of the secondary fuel against main fuel is about 10%. The comparison of spectra among three conditions is shown in Fig.9. In this case, the central frequency for band-pass filter is set to 220 Hz, which corresponds to 1/4 mode. The delay time and open width are set at the value of 0.125 and 0.8 msec respectively. Reduction of peaks by the controls is obvious for all the harmonics. If we focus attention on the highest peaks, it can be seen that more effective reduction was achieved by the closed loop than by the open loop. In Table.1 shows summary of pressure fluctuations and reduction levels. The reduction level is defined by the percentage of the difference of  $p'_{rms}$  between the control on/off against the value of  $p'_{rms}$  when

control off. The reduction levels to the no-control case are 59.7 % for the open loop and 72.3 % for the closed loop.

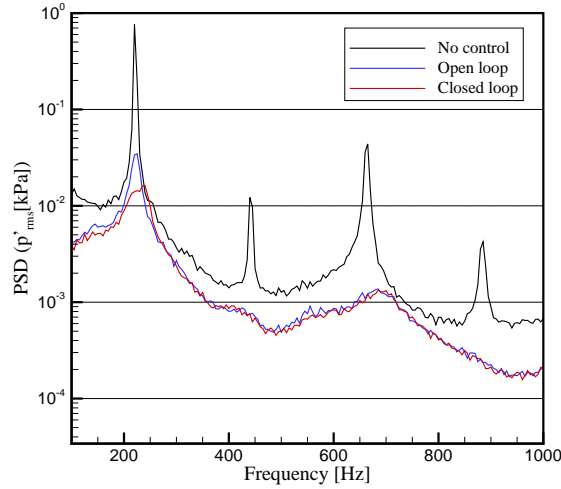


Figure 9: Comparison of power spectra

Table 1: Control effects of secondary fuel injections ( $T_{in}=500K$ ,  $U_{swi}=12m/s$ ,  $L = 810mm$ )

Control	$\phi_t$	SFP [%]	$p'_{rms}$ [kPa]	Reduction [%]	$p'_{rms(peak)}/p'_{rms}$ [%]
No	0.77	0	1.91	—	39.8
Open	0.85	10	0.77	59.7	4.97
Closed	0.85	10	0.53	72.3	3.09

## 4 Open loop control on the higher inlet condition

To simulate more realistically the real gas-turbine combustor, especially on the conditions of inlet temperature and velocity,  $T_{in}=700K$  and  $U_{swi}=90m/s$  were examined next. The chamber length is 484mm in this case. For this condition, the frequencies of the most unstable modes distribute around 500Hz. Since this frequency may be too high for the valve to actuate secondary injection, only open loop control was applied. One possible shortcoming of secondary fuel injection method is that it may increase the emission of NOx. This is severe particularly on highly preheated conditions. Therefore gas sampling measurements were carried out at the exit of the chamber this time.

### 4.1 Characteristics of the combustion oscillation

Acoustic and emission characteristics without control were investigated (Fig.10(a)-10(c)). In this case, the oscillation arose at  $\phi_m \sim 0.60$  and reaches maximum at  $\phi_m \sim 0.62$ . Then it decreases to the level of background in a short range(Fig.10(a)). This was not observed in the former case. The peaks of spectra for pressure show the dominant modes are corresponding to the 1/4 longitudinal acoustic modes of the chamber (Fig.10(b)). In this case, higher frequency modes of oscillation were not clearly observed. The higher value of  $p'_{rms(peak)}/p'_{rms}$ , 78.3% (in table.2), comparing to the value of the former case, 39.8%, supports this trend.

The emissions of NOx and CO are shown in Fig.10(c). The both increase monotonically as equivalence ratio increase. This tendency indicates that complete combustion is achieved over the

range of operation. In other words, it is not the situation that both incomplete combustion and pressure oscillation become key issues at the same time as would be the case of our final target. It is worth describing that there was no clear increment or decrement of emissions due to pressure oscillation in this case.

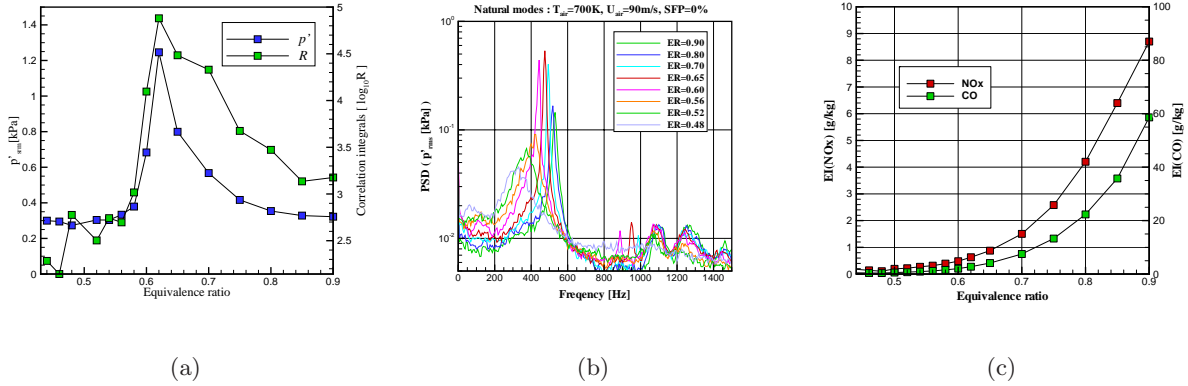


Figure 10: Characteristics of acoustics and emissions (no control) (a)  $p'_{rms}$  and  $R$ , (b) Power Spectra, (c) Emissions of NOx and CO

## 4.2 Effects of secondary fuel injection on pressure oscillation and emission

Open loop control by secondary fuel injection was applied and the effects of fuel percentages were investigated. Fig.11 shows the close-up view of the power spectra around the dominant frequency. In this case, total equivalence ratio was set at a constant value ( $\phi_t = 0.60$ ) and four different percentages, from 1% to 10%, of secondary fuel injections were examined. The evident reductions of peak values are found in all the cases. The reduction levels are summarized in Table.2. Even in the case of the smallest injection, almost 80% of reduction was achieved. Further additions adjust the level to the lower side but in an only small amount.

In order to see the effects on NOx emission, EI(NOx) and the peak values of  $p'_{rms}$  are plotted in Fig.12. What can be imagined readily is the increase of NOx due to the diffusion combustion of the secondary fuel. The resultant emission globally shows the expected trend. However, for the small SFP region, it can be seen that there is a range whose emission level remains in the same level as no fuel injection. These results indicate that there is an optimum amount of secondary fuel injection which effectively works on the reduction both for pressure oscillation and NOx emission. The location of injection is another parameter that can affect much the characteristics and it should be investigated with the detailed optical measurement so as to see the reduction mechanism in detail.

Table 2: Control effects of secondary fuel injections ( $T_{in}=700\text{K}$ ,  $U_{swl}=90\text{m/s}$ ,  $L = 484\text{mm}$ )

Control	$\phi_t$	SFP [%]	$p'_{rms}$ [kPa]	Reduction [%]	$p'_{rms(\text{peak})}/p'_{rms}$ [%]
No	0.60	0	1.61	—	78.3
Open	0.60	1	0.35	78.5	38.1
Open	0.60	2	0.32	80.2	32.0
Open	0.60	5	0.26	83.6	25.5
Open	0.60	10	0.24	85.3	24.6

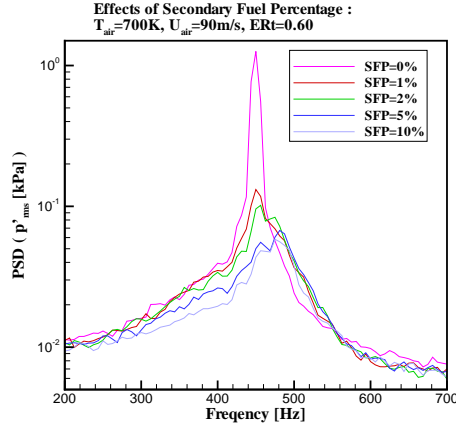


Figure 11: Effect of secondary fuel injection on power spectra

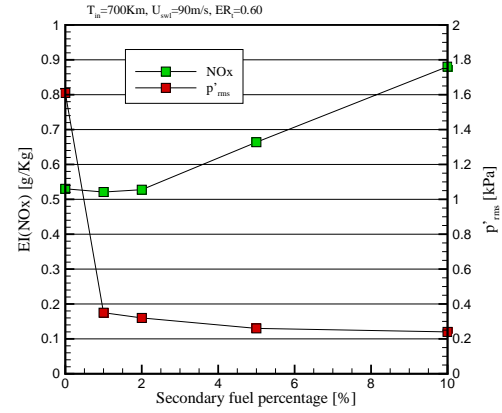


Figure 12: Effect on NOx emission and pressure oscillation

### 4.3 Conclusions

The natural modes of combustion oscillation were investigated for a swirl-stabilized combustor and several means of control were examined. On the condition of  $T_{in} = 500\text{K}$ ,  $U_{swl} = 12\text{m/s}$  and  $L = 810\text{mm}$ , the oscillation begins at  $\phi_m \sim 0.67$  and the frequencies of the highest peaks were found to be the 1/4 longitudinal mode of the chamber. The effects of two methods of secondary fuel injection on the oscillation were examined. The reduction percentages of  $p'_{rms}$  to the no-control case are 59.7 % by the constant injection in the open loop manner and 72.3 % by the pulse injection in the closed loop manner. Hence, in this case, the pulse injection method with the phase-shift approach is considered to be an efficient actuation for the active control of combustion oscillation.

In the similar way, acoustic mode analysis and control trials were carried out on the higher power condition of  $T_{in} = 700\text{K}$ ,  $U_{swl} = 90\text{m/s}$  and  $L = 484\text{mm}$ . In this case, emission properties were investigated also. The open loop control by injecting secondary fuel at constant flow rates reduced pressure oscillation almost 80 % even in a small amount of fuel, for instance 1 % to the main fuel. The NOx emission in the small SFP region were remain the same level as in the case of no injection. It indicates that the structure of the recirculation zone, especially in the region of the flame-anchoring position, is very sensitive to small disturbances and that the small amount of secondary fuel injection has the possibility to greatly affect the heat-release oscillation. Since the amplitude of pressure oscillation is high near the solid wall, for instance the pressure antinode stays at the inlet of the chamber, the correction of heat-release distribution in this region could readily interact with the total acoustic field.

In order to explore robust and effective control methods, more detailed information on the reduction mechanism is needed. For both open and closed loop controls, further investigations especially on the effects of the amount and location of secondary fuel injections will be addressed by optical measurements. Comparison with CFD analysis[12] will also be implemented to the development of the control system.

### Acknowledgement

The authors are pleased to acknowledge the support of the Center for Smart Control of Turbulence, the Ministry of Education, Culture, Sports, Science and Technology of Japan.

## Nomenclature

$I'_{\text{CH}^*}$	: chemiluminescence intensity from CH* radicals	—
$L$	: length of combustion chamber	[mm]
$p'_{\text{rms}}$	: root mean square of pressure fluctuation	[kPa]
$p'_{\text{rms}(\text{peak})}$	: $p'_{\text{rms}}$ of the peak mode	[kPa]
SFP	: secondary fuel percentage against the amount of main fuel	[%]
$R$	: thermo-acoustic correlation integrals	—
$T_{\text{in}}$	: inlet air temperature	[K]
$U_{\text{swl}}$	: bulk velocity of the area of the swirler	[m/s]
$\phi_{\text{m}}$	: equivalence ratio of the main mixture	—
$\phi_{\text{t}}$	: total equivalence ratio	—

## References

- [1] Candel,S., *Proc. Combust. Inst.* 29:1-28(2002).
- [2] Lee,J.G. and Santavicca,D.A., *Journal of Propulsion and Power*, 19:735-750 (2003).
- [3] Lee,J.G., Kim,K., and Santavicca,D.A., *Proc. Combust. Inst.* 28:739-746 (2000).
- [4] McManus,K.R., Vansburger,U., and Bowman,C.T., *Combust. Flame*, 82:75-92 (1990).
- [5] Paschereit,C.O., Gutmark,E., and Weisenstein,W., *Combust. Sci. and Tech.*, 138:213-232(1998).
- [6] Prasanth,R.K., Annaswamy,A.M., Hathout,J.P., and Ghoniem,A.F., *Journal of Propulsion and Power*, Vol.18, No.3, 658-668 (2002).
- [7] Zimmer,L., Tachibana,S., Yamamoto,T., Kurosawa,Y., and Suzuki,K., in *Proceedings of the 4th symposium on smart control of turbulence, Tokyo*, March 2-4, 2003, pp 93-102.
- [8] Zimmer,L., Tachibana,S., in *Proceedings of the 5th symposium on smart control of turbulence, Tokyo*, February 29 - March 2, 2004.
- [9] Tanahashi,M., Nada,Y., Tsukinari,S., Saitoh,T., Miyauchi,T. and Choi,G-M., in *Proceedings of the 4th symposium on smart control of turbulence, Tokyo*, March 2-4, 2003, pp 81-91.
- [10] Hayashi,A.K., Sato,H., Endo,T., Yasunami,Y., Yoshimi,S., Ikame,M., Kishi,T., Hiraoka,K., Harumi,K., and Oka,H., in *Proceedings of the 4th symposium on smart control of turbulence, Tokyo*, March 2-4, 2003, pp 173-182.
- [11] Shinjo,J., Mizobuchi,Y. and Ogawa,S., in *Proceedings of the 4th symposium on smart control of turbulence, Tokyo*, March 2-4, 2003, pp 165-172.
- [12] Shinjo,J., Mizobuchi,Y. and Ogawa,S., in *Proceedings of the 5th symposium on smart control of turbulence, Tokyo*, February 29 - March 2, 2004.